

## FATIGUE PROPERTIES OF THIN WALL SEMI-PRODUCTS PRODUCED BY INCREMENTAL FORMING PROCESSES

Masek, B.; Malina, J.; Cerny I.; Ciper M.; Hronek, P.; & Jenicek, S.

**Abstract:** *The actual tendencies lead to the improvement of current technologies, search for new methods, or use of known technologies in other ways. In this case, the flow forming process for reducing the diameter of thick-walled hollow semi-products was used. Flow forming is one of the progressive technologies which use incremental deformations for achieving the required aims. With this technology the stepped hollow semi-products were produced.*

*The research was firstly focused on determining the influence of forming conditions on the structural and mechanical properties of the final product. The mechanical properties were established on the mini tensile test. Consequently, the final product fatigue properties were observed on the small segments from each part of the final product.*

*Key words: fatigue, flow forming, microstructure, mechanical properties.*

### 1. INTRODUCTION

Flow forming [1, 2, 3] uses three rollers for the reduction to final diameters.

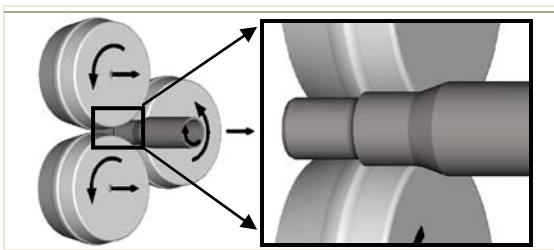


Fig. 1. The scheme of the principle of flow forming

These three rollers are not driving and their rotation is attained through the friction between the wrought rotating semi-product and the shaping rollers Fig. 1.

The experiment was focused on the examination of influence of the forming process on structural and mechanical properties of final product.

### 2. THE INITIAL SEMIPRODUCT

The material of the initial thin wall semi-product used in the experiment was the low alloyed steel 16MnCrS5 (Table 1). The initial diameter of the semi-product was 60 mm and wall thickness 6 mm. The material in the base state had the ferrite – pearlite structure and an average grain size of about  $10\pm 5 \mu\text{m}$  Fig. 2.

| Element | C    | Si  | Mn  | Cr | S    | P    |
|---------|------|-----|-----|----|------|------|
| [%]     | 0.16 | 0.4 | 1.2 | 1  | 0.03 | 0.03 |

Table 1. Chemical composition of steel 16MnCrS5

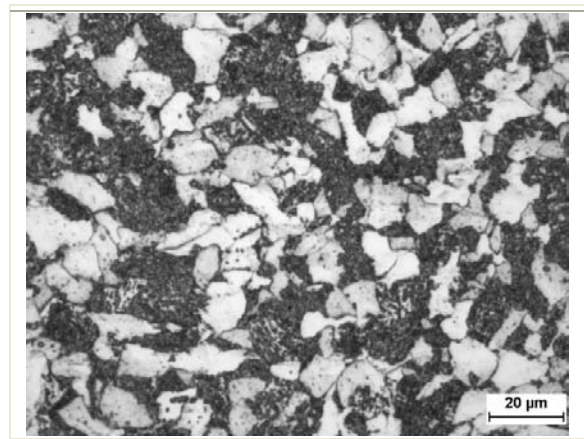


Fig. 2. The initial ferrite-pearlite structure

| Rod [mm] | R <sub>m</sub> [MPa] | R <sub>p02</sub> [MPa] | A <sub>5mm</sub> [%] | Z [%] |
|----------|----------------------|------------------------|----------------------|-------|
| Ø 60     | 687                  | 680                    | 23                   | 64    |

Table 2. The mechanical properties of the material in the initial state (Fig. 17)

The mechanical properties of the initial material exhibited relatively low ductility 23% and higher yield strength 680 MPa. The ultimate strength was 687 MPa (Table 2) and micro-hardness 238 HV 0.2.

## 2. EXPERIMENT

Because of the lower formability of initial material, the semi-products were soft annealed at 700°C for 180 min before the forming experiment. As a result of this soft annealing the ferrite-pearlite structure with the spheroidal cementite was formed Fig. 3, with micro-hardness 157 HV 0.2 and ductility higher than 40% (Table 3).

The structure with these structure-mechanical properties provided the sufficient formability for the forming.

### 2.1 THE FLOW FORMING

The flow forming was carried out on the machine developed for incremental forming processes. The forming was made at room temperature with the feed speed 2 mm/rev. The thin wall semi-products were formed from the base size Ø 60 mm to Ø 45 mm and then to Ø 40 mm, Fig. 4.

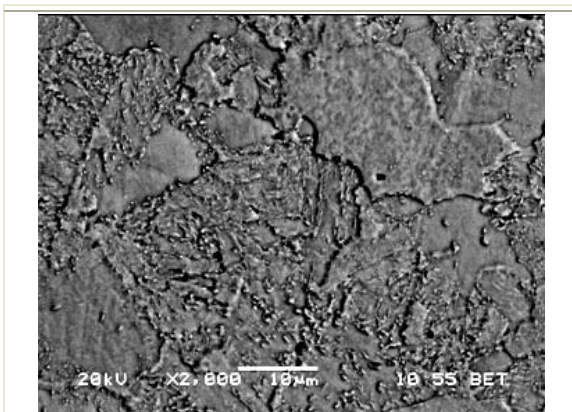


Fig. 3. The ferrite-pearlite structure with spheroidal cementite

| Rod [mm] | R <sub>m</sub> [MPa] | R <sub>p02</sub> [MPa] | A <sub>5mm</sub> [%] | Z [%] |
|----------|----------------------|------------------------|----------------------|-------|
| Ø 60     | 480                  | 316                    | 44                   | 79    |

Table 3. The mechanical properties of the material after the soft annealing (Fig. 17)

In the next step were the products shot peened in order to increase fatigue properties.

For the purpose of metallographic analysis were the products cut in several parts and the influence of size reduction on the microstructure was observed in the whole cross-section of the thin wall product.

With the help of light microscopy it was possible to observe the distribution of deformation in the formed structure.

The ferrite-pearlite structure observed in the part reduced to Ø 45 mm was strongly deformed in the direction of the rollers rotation Fig. 5. The spheroidal type of cementite provided higher formability of the structure and it was concentrated mainly in the surface area.

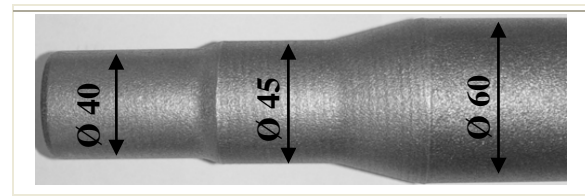


Fig. 4. The shape of final product after the flow forming

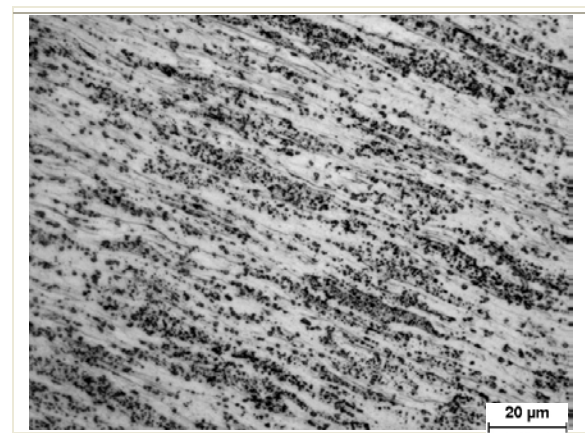


Fig. 5. The structure after reduction to Ø 45 mm in the distance 0.25 mm from the surface

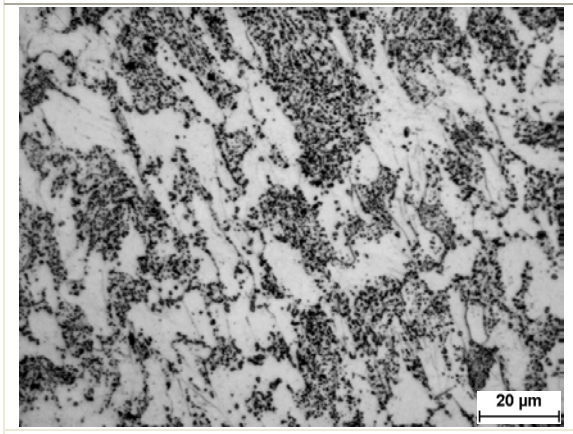


Fig. 6. The structure after reduction to  $\varnothing$  45 mm in the middle of the wall

With the growing distance from the surface the size of deformation decreased. In the middle of the product wall the structure was only gently deformed especially in the ferrite area Fig. 6.

The highest deformation in the whole volume of the product was achieved in the area of semi-product reduced to the smallest size of 40 mm diameter. Especially in the under-surface zone Fig. 7 the structure showed marked deformation and the deformed grains were practically parallel to the product surface.

The pearlite area in the part reduced to 40 mm diameter underwent higher deformation in comparison with the part reduced to diameter 45 mm.

But even the reduction to the 40 mm didn't result in a homogeneous deformation

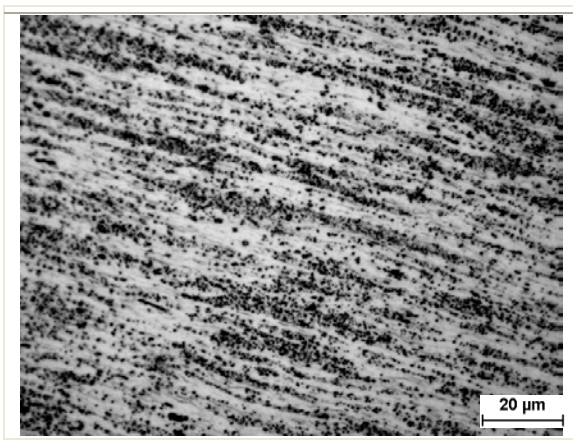


Fig. 7. The structure after reduction to  $\varnothing$  40 mm in the distance 0.25 mm from the surface

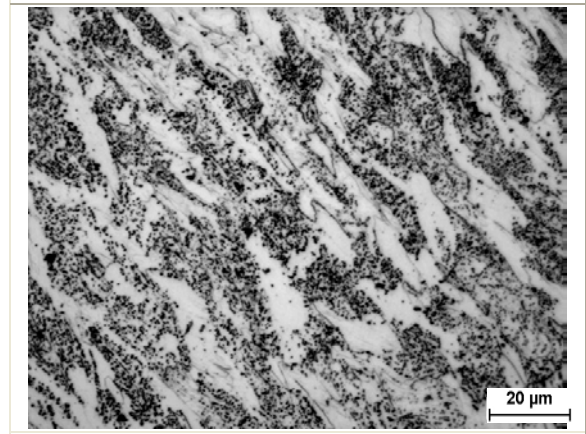


Fig. 8. The structure after reduction to  $\varnothing$  40 mm in the middle of the wall

distribution in the whole wall size of the product and the middle part of the product was again less deformed in comparison with surface Fig. 8.

In the next step, the mini-tensile tests were made from each part of the product.

The results showed an increased  $R_m$  by about 140 MPa in the area of  $\varnothing$  45 mm or by 160 MPa in area of  $\varnothing$  40 mm. The increase of  $R_{p02}$  was higher than 300 MPa in both formed parts. The residual ductility was higher than 25% (Table 4).

## 2.2 THE HEAT TREATMENT

Because this material is commonly used in the cemented state, the hollow stepped products were subsequently carburized. This heat treatment consists of preheating at temperature  $910^{\circ}\text{C}$  and 140 min hold on this temperature with carbon concentration 1.1%. Then was the concentration of carbon reduced to 0.8% and the hold time was 45 min. After that, the carburizing temperature was decreased to  $860^{\circ}\text{C}$  with carbon concentration 0.75% for 45 min.

| Diameter [mm]    | $R_m$ [MPa] | $R_{p02}$ [MPa] | $A_{5mm}$ [%] | Z [%] |
|------------------|-------------|-----------------|---------------|-------|
| $\varnothing$ 45 | 624         | 623             | 24            | 71    |
| $\varnothing$ 40 | 646         | 644             | 26            | 71    |

Table 4. The mechanical properties of the material after the soft annealing (Fig. 17)

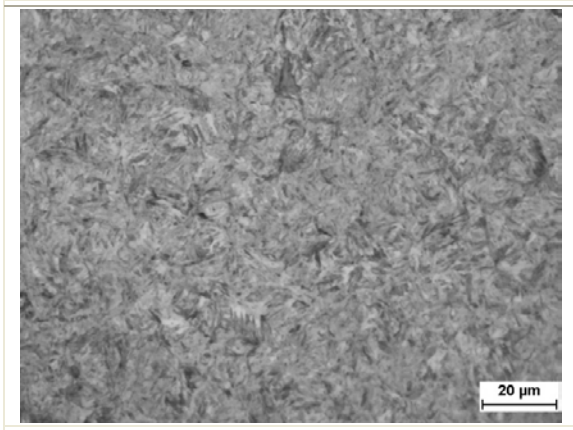


Fig. 9. The martensitic structure in the surface layer

In the last step, the final products were quenched in oil and at the end were the heat treated products tempered at 170°C for 2 hours.

The metallographic analysis of the product showed that after heat treatment combined with carburization was achieved the uniform martensitic structure, both in the surface layer Fig. 9 and also in the middle of the wall of product Fig. 10. The martensite in the structure was in the needle form.

For the next evaluation of carburization process it was necessary to determine a carburized depth. For this purpose the micro-hardness was measured. The micro-hardness load was 1,96 N and the micro-hardness profile was measured from the outside surface to the middle section of the wall with 0.1 mm step, Fig. 11.

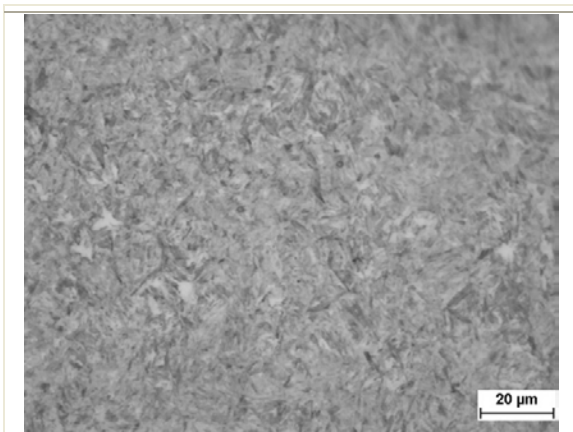


Fig. 10. The martensitic structure in the middle of the wall

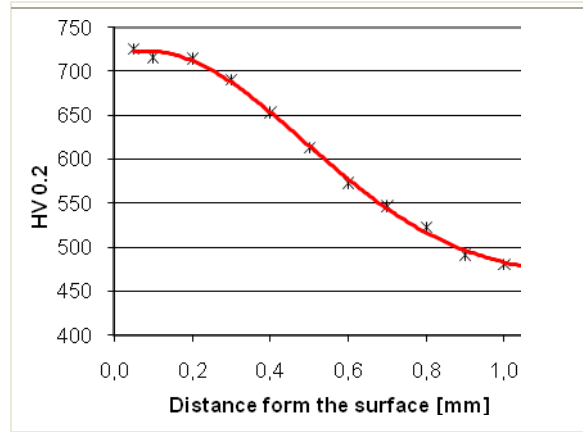


Fig. 11. Profile of hardness in carburized depth

The results documented that the carburized depth corresponded to aimed thickness of about 0.9 mm Fig. 11.

The mechanical properties of final carburized products were established with the mini-tensile test. The mini-tensile specimens were cut off from each diameter of the product.

The results of this tests proved that the previous forming didn't influence the mechanical properties of final product. The ultimate strength was in each diameter c. 1350 MPa. The yield strength was around 1235 MPa and the ductility  $A_{5mm}$  was higher than 20% (Table 5).

### 2.3 THE FATIGUE TESTS

The last part of the experiment was focused on the review of fatigue properties of final-product. The specimens for the fatigue tests were divided into four groups.

In the first group were specimens obtained from the initial diameter of the product with the carburized surface. The second group consisted of specimens acquired

| Diameter [mm] | $R_m$ [MPa] | $R_{p0.2}$ [MPa] | $A_{5mm}$ [%] | Z [%] |
|---------------|-------------|------------------|---------------|-------|
| Ø 60          | 1358        | 1235             | 22            | 58    |
| Ø 45          | 1347        | 1240             | 21            | 57    |
| Ø 40          | 1355        | 1230             | 21            | 57    |

Table 5. The mechanical properties of material after heat treatment

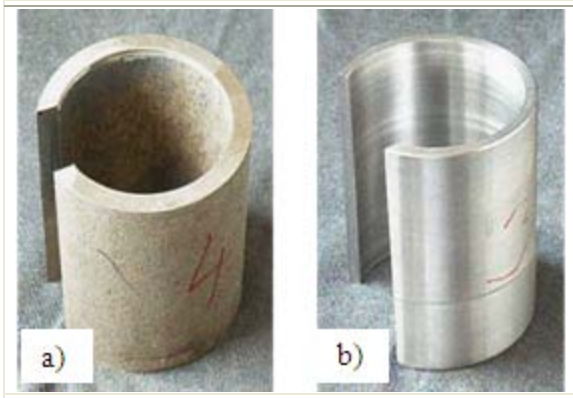


Fig. 12. The initial diameter of the product with a) and without the carburized layer b)

from the initial diameter of product but the cemented surface was removed prior to fatigue test Fig. 12.

The third group of specimens was obtained from the mean diameter of product and it was with the carburized surface, while in the last group were specimens taken from the same part but the cemented surface was removed again.

The fatigue tests were carried out with the help of three-point bending test Fig. 13.

The size of specimens in the middle part was about 8 mm and for the higher accuracy it was controlled after the test Fig. 14. Each sample was measured using strain gauge.

The specimens with removed carburized surface and formed to  $\varnothing 45$  mm had stress range corresponding to the fatigue limit 1250 MPa, while the specimens from unformed part reached only 1000 MPa Fig. 15.

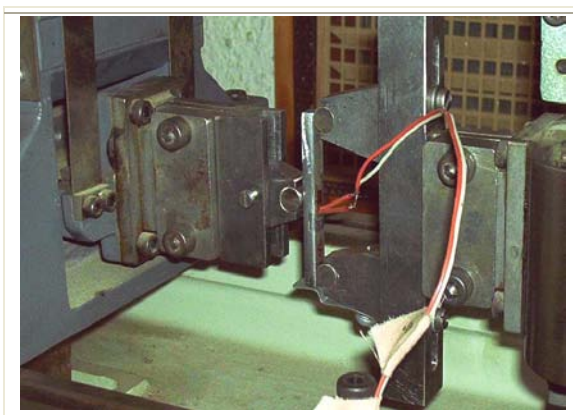


Fig. 13. The testing machine for three-point bending test

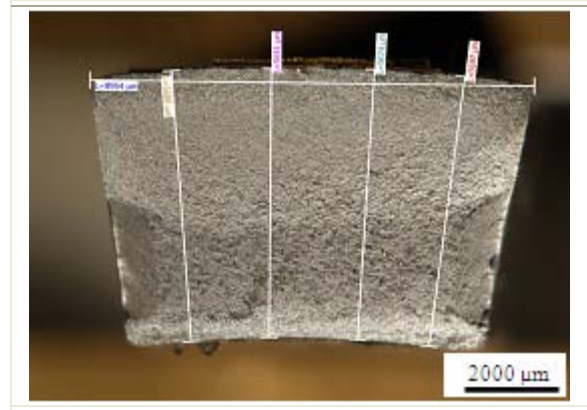


Fig. 14. The exact measurement for estimation real load in the test specimen

On the other hand, the samples with carburized surface layer didn't show significant difference in the fatigue limits between formed and undeformed parts of final product and the stress range corresponded with the fatigue limit 700 MPa.

Most of the samples exhibited the initiation of fatigue cracks on the structure impurities.

In the case of the samples formed to  $\varnothing 45$  mm it was observed that the fatigue cracks initiated not only on the metallurgical impurities, but also on the micro-defects caused by forming on the surface of semi products Fig. 16.

### 3. CONCLUSION

The results of the experiment verified the possibility to produce the praxis relevant products for the light-construction

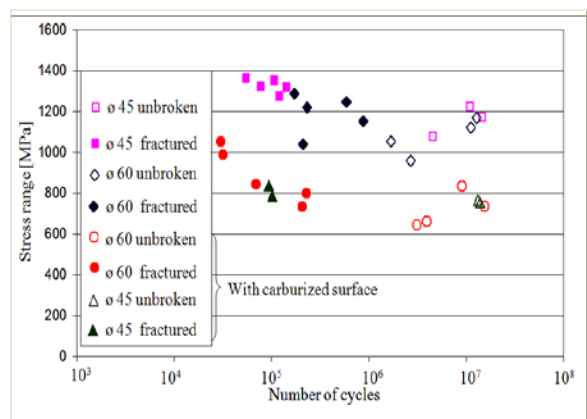


Fig. 15. Results of the fatigue tests on the final product

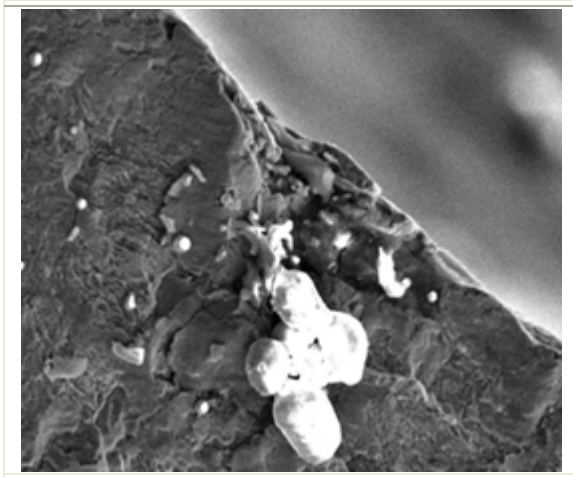


Fig. 16. The initiation of the fatigue crack on the defect in the surface layer

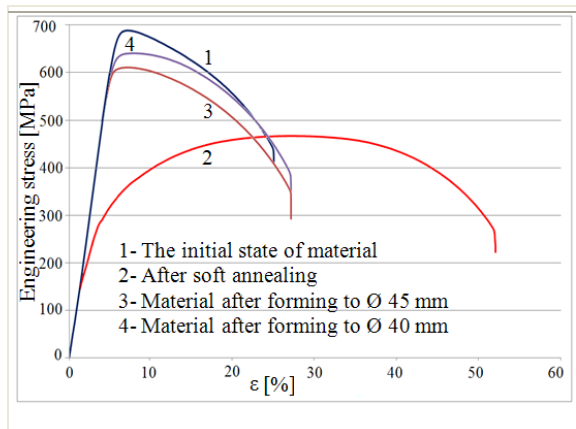


Fig. 17. Development of mechanical properties – tensile test

area by technological change with integrated flow forming process mentioned above.

In the incrementally formed part of the products, was with the help of this technology achieved the increase of yield strength in average about 100% Fig. 17.

On the base of the results of the fatigue tests, it was possible to estimate the range of the usage of final products in the praxis. The stress range relating to the fatigue limit was in all of the cases higher than 650 MPa. The highest fatigue limit 1250 MPa was determined in a part of the specimens formed to Ø 45 mm with removed carburized surface layer. This result of the fatigue limit corresponds to the loading

cycle with stress amplitude of 625 MPa and the cycle asymmetry 0.1.

#### 4. REFERENCES

1. Awiszus, B. Meyer, F. Meyer, L.W. Hahn, F. *Erweiterung der Formgebungsgrenzen durch inkrementelle zyklische Umformung am Beispiel des Drückwalzens (Abstreckdrücken)*. Tagungsband zum Abschlusskolloquium des DFG Schwerpunktprogramms 1074 „Erweiterung der Formgebungsgrenzen bei Umformprozessen“, Aachen, 3. Mai 2005.
2. Awiszus, B. & Meyer, F. (2006) *Der Einfluss technologischer Kenngrößen und Parameter auf den quasistationären Zustand beim Drückwalzen – Beschleunigung der FEM durch modifizierte Anfangswerte*. Zwischenbericht im DFG Schwerpunktprogramm 1146 „Modellierung inkrementeller Umformverfahren“, Chemnitz, Oktober 2006.
3. Ufer R., (2006). *Modellierung und Simulation von Drückwalzprozessen* Dissertation, Verlag Wissenschaftliche Scripten, 2006. ISBN-13: 978-3-937524-43-6.

#### 5. ACKNOWLEDGEMENTS

This paper includes results created within the project IM06032 Research Centre of Forming Technology and within the project P107/10/2272 Accelerated Carbide Spheroidization and Grain Refinement in Steels. The projects are subsidised from specific resources of the state budget for research and development.

#### 6. ADDITIONAL DATA ABOUT AUTHOR

Malina, Jiri, mali@centrum.cz, Zapadoceska univerzita v Plzni, Vyzkumne centrum tvarecich technologii, Univerzityni 22, P.O. Box 314, CZ - 306 14 Plzen